TIME-DEPENDENT INTERACTION BETWEEN CARBON-BONDED ALUMINA FILTERS AND MOLTEN STEEL

Anne Schmidt[1], Steffen Dudczig[1], Anton Salomon[2], Tilo Zienert[2], Enrico Storti[1], David Rafaja[2], Christos G. Aneziris[1]
[1]TU Bergakademie Freiberg, Institute of Ceramic, Glass and Construction Materials, Freiberg, Germany
[2]TU Bergakademie Freiberg, Institute of Materials Science, Freiberg, Germany

ABSTRACT

Understanding reactions between filter material and molten steel is essential to improve the purity of casted products by filtration. This contribution illuminates the kinetics of interactions between carbon-bonded filters and molten steel. In addition, a thermodynamic model complements the experimental results to describe the impact of carbon on these reactions. For the experiments, carbon-bonded alumina filters were coated either with pure alumina or with a mixture of alumina and 4 wt.% carbon (Al_2O_3+4C). Two methods were applied to evaluate the time dependence of the interactions. First, long-time experiments up to 30 min were carried out using spark plasma sintering (SPS) equipment. In the SPS tests, the flow of molten steel is minimized that allows an almost undisturbed examination of the chemical reactions at the interface. Secondly, the coated filters were immersed in molten steel for 10 s up to 120 s. These short-time tests were performed using a special steel casting simulator providing close-to-reality conditions. The phase composition and the distribution of phases at the metal/ceramic interface were characterized by means of optical microscopy, scanning electron microscopy (SEM) with energy and wavelength dispersive X-ray spectroscopy (EDX and WDX), and electron backscatter diffraction (EBSD). Carbon seem to accelerate the layer buildup during steel contact, as the in situ formed layers were more pronounced after immersing filters coated with Al_2O_3+4C for 10 s into the molten steel compared to pure alumina coated ones. The long-term SPS experiments also revealed enhanced chemical interactions of Al_2O_3+4C coated filters. The findings indicate that an accelerated dissolution and precipitation of alumina from steel is triggered by the presence of carbon, which is in excellent agreement with predictions obtained from the thermodynamic model. Interestingly, very fine inclusions having the size of a few micrometers were found on the surface of alumina coated filters after 60 s and even more of these inclusions after 120 s immersion. They are probably deposited directly from the molten steel. In summary, the carbon content of alumina based filter material significantly influences the steel melt filtration. The thermodynamic model clarified the impact of carbon on these interactions and will be beneficial to tailor future filter material compositions.

Keywords: Steel melt filtration, carbon-bonded alumina, ceramic foam filter

INTRODUCTION

Non-metallic inclusions embedded in cast metal parts remarkably impair their performance. In particular the size, kind, density and distribution of non-metallic inclusions in metals are well known to influence their mechanical properties. Especially fracture toughness, tensile strength, ductility and fatigue of the products are affected, which can result in excessive casting repairs or rejected products. [1–3]

For decades, ceramic foam filters have successfully been applied in iron and aluminum melt filtration. [4] In the case of steel melt filtration, filters based on partially stabilized zirconia or carbon-bonded alumina have been used. [2,4]

Within the framework of the Collaborative Research Center (CRC) 920, carbon-bonded alumina filters are investigated in detail to improve their filtration performance, for example by applying functional coatings. [5,6] Studies of Storti et al. [7,8] and Poirier and Thillou [9] indicate that the amount of carbon strongly influences the interactions between carbon-bonded alumina and molten steel. This study illuminates the influence of carbon regarding the time-dependent behavior of coated carbon-bonded alumina filters and molten steel.

In this study, two approaches were applied. For the first one, SPS equipment was used. Thereby, a filter sample and steel powder were heated up with extremely high heating rates (up to 1300 K min^{-1}), and the final temperature was held for either 1 min or 30 min. This set-up minimized the macroscopic flow of molten steel. As a result, chemical reactions at the interface between the functionalized filter surface and the metallic melt were examined that were almost unaffected by mechanical attack or interlocking of inclusions on the filter surface. [10]

The second series of experiments involved immersion tests that were carried out with immersion times ranging from 10 s to 120 s using a steel casting simulator. Due to the inductive heating, a flow within the melt was created in such a way that the melt streamed on the rotating filter. After immersion, the filter was cooled down in an argon floated chamber in order to prevent oxidation during cooling, but also to drip off the steel melt from the filter surface. The latter made the analysis of the interfacial reaction products on the filter surface easier. This represents a big advantage as compared to real filtration tests, after which the solidified steel usually remains in the filter and complicates a detailed analysis of the interfacial reaction products.

From our results, we deduce a more detailed model of the interactions between alumina coated carbon-bonded alumina filter and Al-killed steel. If a sufficiently high amount of carbon is present at the filter/steel interface, the filter behaves “reactively” due to dissolution and precipitation processes of alumina. As soon as the carbon supply is interrupted, these interfacial reactions come to an end and endogenous inclusions are deposited on the “actively” acting filter.

MATERIALS AND METHODS

Filter Manufacturing

Manufacturing the ceramic foam filters is commonly based on the processing route patented by Schwartzwalder and Somers in 1963 [11]. The examined filters were produced following the same routine as described by Emmel and Aneziris [12]. Thereby, the carbon-bonded alumina filters were generated in two steps. First, polyurethane templates were impregnated with a water-based carbon-alumina slurry. Secondly, they were spray coated to the final wet weight of 26 g (± 1 g). Impregnation slurry and spray-coating slurry were of the same composition except for the solids content. The slurries were based on composition no. 3 in [12], which was further optimized by Emmel [13]. Due to agglomeration issues, the alumina raw material MR 70 was pretreated in the same way as described by Storti et al. [8] and Fruhstorfer et al. [14]. The prepared filters were heated up to 800 °C under reducing atmosphere following the temperature program presented in Ref. [12]. Afterwards, the alumina coating was applied as a thin layer (about 20 µm to 100 µm) by cold spray coating. The composition was based on the alumina coating presented in Ref. [5]. To improve the slurry stability for the Al_2O_3+4C composition, though the alumina powder CL 370 was partially replaced by the finer MR 70 (ratio 25:75). Furthermore, 6.25 wt.% of alumina were replaced by Carbores P in composition Al_2O_3+4C. That resulted in a residual carbon content of 4 wt.% after the heat treatment. The spray coating

process and the following heat treatment up to 1400 °C were similar to that described by Emmel and Aneziris [5].

Interface Reaction in Spark Plasma Sintering Tool

Samples of the coated filters and a powder of the steel grade 42CrMo4 were heat-treated in an SPS unit HPD 25 (FCT Systeme GmbH, Germany). The setup was similar to the procedure described by Salomon et al. [10]. Hollow ceramic cylinders made of the carbon-bonded alumina filter material served as sintering molds. They were filled with steel powder and pieces of the coated filter. Bottom and top of the hollow cylinders were covered by sheets of the carbon-bonded alumina to avoid leakage of the molten steel. This assembly was placed in the graphite tools of the SPS.

All SPS experiments were carried out in power controlled heating mode to achieve the highest possible heating rate of about 1300 K min^{-1} from 450 °C to a final temperature of 1600 °C. The original working pressure of 0.5 Pa increased to 5 Pa upon heating and chemical reaction producing carbon oxides. After dwell times of 1 min or 30 min, the heating was switched off, and the samples were rapidly cooled by water-cooled steel electrodes.

Immersion Tests

The immersion tests were carried out using a special steel casting simulator (SCS). Therein, about 30 kg of a steel grade 42CrMo4 were melted within alumina-spinel crucibles. These crucibles were produced only for these experiments to avoid any CaO impurities, which may react with inclusions of the steel. The crucible composition, further process parameters and the immersion test cycle were the same as described by Dudczig et al. [6]. The short immersion trials of 10 s and 30 s were performed in accordance to Storti et al. [8]. Additionally, the immersion times were extended to 60 s as well as 120 s. The pretreatment of the steel ensured that each immersion trials started at similar oxygen levels. Thereby, the dissolved oxygen content and the temperature of the steel were determined after each stage of the trials: melting of the steel, oxidation with 0.5 wt.% iron oxide, deoxidation with 0.05 wt.% aluminum, and after the filter immersion.

Characterization of the filter and metal samples

Before and after the SPS trials, local chemical analyses of the cross-sectional interfaces of the polished samples were carried out using a high-resolution scanning electron microscope (SEM) LEO-1530 (Carl Zeiss AG, Germany) with a field emission cathode and an energy dispersive X-ray (EDX) detector (Bruker AXS).

The microstructure of the samples before and after the immersion tests was characterized by light and electron microscopy. For light microscopy, a digital light microscope VHX-2000 D (Keyence, Germany) equipped with an objective VH-Z20R was used. Carbon-sputtered samples were prepared and analyzed by an electron microscope Philips XL 30 (Phillips, Germany), which was also equipped with an EDX detector (EDAX-Ametek, USA).

An SEM of the type Versa3D (FEI Company, USA) that was equipped with electron backscatter diffraction (EBSD) and EDX (both from EDAX-Ametek, USA) was used to determine the phase composition of deposited particles.

RESULTS AND DISCUSSION

SPS sample treatment

After the SPS heat treatment, solidified steel persisted on the filter samples. After the dwell for one minute at the final temperature, microstructural changes of the carbon-bonded alumina nearest to the coating were observed for both filter types. In addition, bright spots were detected in BSE micrographs in that area. They contained iron and main alloying elements as determined by EDX. Thus, some steel might have moved through the coating material and have contributed to these microstructural changes. Similar observations have been done on coated and uncoated Al_2O_3-C filters. [6] According to them, these changes resulted from decarburization that had been triggered by iron acting as catalyst. Despite some cracks, which were probably caused by the strong thermo-shock, no distinct changes were observed at the coating/steel interface after one minute testing time. After 30 minutes (Fig. 1), however, the decarburization of the carbon-bonded alumina material was more pronounced and this zone became thicker. Unsurprisingly, the alumina in the coating was sintered with increasing testing time. Additionally, some particles near the coating surface were detected. EDX indicated that these particles consisted of aluminum and oxygen in the ratio of Al_2O_3. Further, line scans by WDX reveal that the steel near the filter surface is enriched with aluminum.

For all observations, the outcome was more pronounced or enhanced for the Al_2O_3+4C coated filter, i.e. the decarburized zone, the formation of alumina structures on the filter surface, the amount of aluminum in steel near the filter.

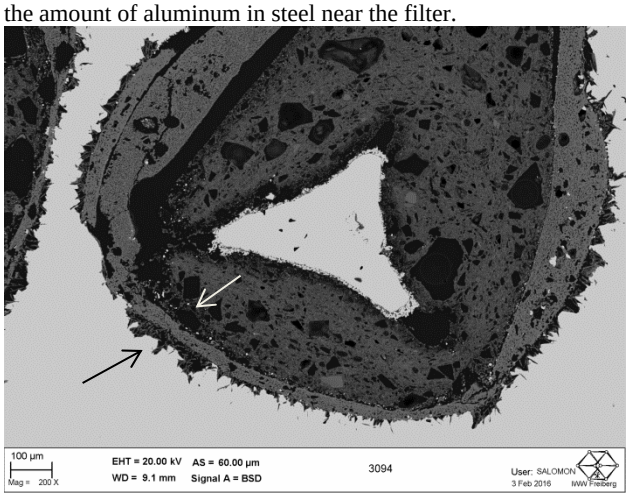

Fig. 1: Cross-section of the Al_2O_3 + 4%C coated filters after the 30 min heat treatment in SPS. The micrograph was taken in the BSE mode. White arrow: decarburized zone; black arrow: formed alumina structures.

Immersion trials

The scheme in Fig. 2 exemplifies the observed layer buildup on the filter surface after immersing an alumina coated filter in molten steel.

In the case of the alumina coated filters, a new layer on top of the alumina coating was observed. Small, mostly plate-like structures were in an initial state of growth. Comparing 10 s and 30 s immersed filters, larger structures were formed. The solidified steel was also detected between them. After 60 s, in addition to that layer with plate-like structures, fine clusters were attached on top of these crystals in some areas on the investigated filter surface. These clusters completely covered the filter surface after 120 s immersing.

Similar to the SPS experiments, a decarburized area and steel droplets were observed in the carbon-bonded alumina material under the coating of immersed filters. However, this zone was not as pronounced as in the SPS-samples.

The newly formed layer was only a few hundred nanometers thick. The analyzed sections indicated that this layer was amorphous and contained tiny crystals. Traces of Si and Ca were detected in that layer.

Alumina structures, which formed on the filter surface, were mostly plate-like and more crowded – bush-likely – near remaining steel droplets. They consisted of polycrystalline corundum having the size of 50 µm. There was no apparent orientation relationship between the attached crystals and the

alumina grains in the coating. Most probably, these crystals originated from heterogeneous nucleation at the filter/steel interface. Furthermore, the grain size of the polycrystalline structures was comparable with the size of endogenous inclusions [15]. Hence, they may have also contributed to their formation.

The observed clusters had a size smaller than 5 µm and consisted of nanometer sized particles. Their morphology closely investigated by SEM is in excellent agreement with reports of endogenous inclusions that originate from aluminum killing during steelmaking [15] and component failure that was traced back to alumina inclusions [3].

If 4 wt.% carbon remain in the alumina coating, the layer structure was basically the same. However, after 10s immersion the formed alumina structures were already longer (about 10 µm to 20 µm). In addition, another up to 2 µm thick layer was found locally that covered the filter surface and the alumina structures. Combined EBSD and EDX analyses indicated that this layer was completely amorphous and contained higher amounts of Si and Ca, and minor amounts of Na. After 60 s and 120s, this layer was not observed. In contrast to the alumina coated filters, no clusters were observed at the filter surface. Further, the alumina structures became rounder the longer the immersion time.

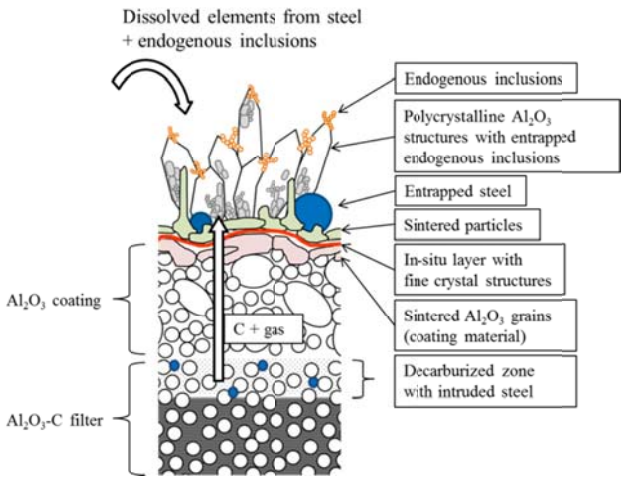

Fig. 2: Scheme of the formed layers buildup on an alumina coated filter surface. Underneath the alumina coating, the carbon-bonded filter was decarburized. Within that zone, some steel droplets were observed. The outer alumina grains of the coating sintered due to the steel melt temperature (1650 °C). On top of the alumina coating, a thin, in-situ formed layer was observed. Due to the interfacial reactions, polycrystalline plate-like alumina structures were formed from heterogeneous nucleation. Likely, not only gases from the decarburized filter material and dissolved elements of the molten steel were involved in their formation, but also endogenous inclusions from the steel melt. They sintered with increasing immersion time as well. Steel got entrapped between these structures. Finally, endogenous inclusions were deposited on the platelets.

DISCUSSION

A layer buildup on the filter surface resulting from interfacial reactions between filter and steel were observed (Fig. 2). Thereby, a thin layer was firstly formed on the filter surface, which seems to be at least partially amorphous. The amorphous phases may form due to impurities of Ca and Si, which should have originated from the raw materials, and can form phases with a low melting point.

The non-related grain orientation of the alumina structures regarding the alumina grains of the coating supports heterogeneous nucleation as origin of these particles. Deposited endogenous inclusions from the steel might serve as nuclei, too.

Thermodynamic studies of Zienert et al. [16] described the layer build-up on immersed carbon-bonded filters, which were prepared by Dudczig et al. [6]. They suggested that alumina of the filter dissolve partially in molten steel. Carbon accelerates this reaction, which is in accordance to the discussion of Poirier et al. [9] regarding clogging mechanism on submerged entry nozzles (Al_2O_3-C). Further, Zienert et al. [16] showed that the argon atmosphere influences the stability of the carbon-bonded alumina, despite it is an inert gas. Thereby, Al_2O_3-C partially decomposed and promoted the formation of gaseous phases containing Al, C, and/or O, and aluminum oxocarbides.

The current thermodynamic model considers the elements Al, Fe, O and C. Nevertheless, also the other elements and oxides, like SiO_2, alkali and earth alkali elements will affect the interactions between filter and steel melt. As an example, Poirier et al. [9] described the formation of a vitreous phase containing Al_2O_3, SiO_2, and alkalis. That phase should have originated from impurities of the refractory, whereby SiO_2, Na_2O, K_2O were reduced by carbon of carbon-bonded refractory. As mentioned above, they also explained the formation of plate-like alumina crystals on the filter surface as a result of dissolution and precipitation of alumina in/from molten steel. According to them, dissolved carbon of the refractory increased the activity of aluminum in molten steel and hence accelerated the alumina dissolution. Lee et al. [17] described a FeO formation as starting point for their interfacial reactions between carbon-bonded alumina refractory and an Al killed steel. Thereby, SiO_2 and FeO in that initial layer were reduced by Al, which was dissolved in molten steel. That lead to the formation of hercynite and finally to the formation of alumina.

In addition, we deduce from our results that carbon contained in the carbon-bonded alumina had an essential influence on the interfacial reactions between filter and steel melt due to the microstructural changes within the carbon-bonded alumina filter we observed. Thereby, the mechanism may be similar to the mechanism described in literature. Due to the porous coating, gaseous reaction products from the carbon-bonded alumina could easily move to the filter/steel interface. Carbon containing gases may be reduced by aluminum in steel and enhanced the alumina dissolution on the other hand. As the system was out of equilibrium, alumina may have precipitated again at the filter surface due to a changing oxygen activity within the melt.

Consequently, two mass transports should have contributed to the layers buildup on the filter surface. These two are, on the one hand, gaseous reaction products (e.g. CO, alumina sub-oxides, and/or Al-O-C gas species) originating from the carbon-bonded material underneath, and endogenous inclusion as well as dissolved elements from the steel, on the other hand.

Nonetheless, after the initial layer and alumina polycrystal formation, in the case of alumina coated filters after 30 s immersion, neither a distinct thickening of the in-situ layer nor an increase in the polycrystal size was observed. If we consider that with increasing immersion time, sintering of alumina near the interface proceeded, it is reasonable to assume that fewer gaseous products from the carbon-bonded filter may have reached the filter/steel melt interface with increasing immersion time. Thus, the dissolution/precipitation processes slowed down. Here, that should be the case between 30 s and 60 s for the alumina coated filters.

Now, endogenous inclusions from the steel melt should be mainly attracted by the alumina platelets, i.e. by the same chemistry. [18]

Such a change was not observed for Al_2O_3+4C coated filters. On the one hand, the increased amount of carbon clearly promoted the alumina polycrystal formation as shown as well in the SPS as in the immersion experiments. However, the increase of carbon in the coating is also accompanied by an enhance amount

of impurities. As above explained by Poirier et al. [9] and Lee et al. [17], the impurities influenced the formation of a vitreous layer on the filter surface. Thereby, a thicker layer covering the alumina polycrystals was found in addition to the in-situ layer on the coating (compare Fig. 2). As the thicker layer was not observed any longer after 60 s immersions, its components might have been reduced during the interactions. Further, the sintering of the filter surface was accelerated for this filter type. If that affected the deposition of endogenous inclusions, cannot be stated at the present, but will be clarified in future investigations.

CONCLUSION

Time-dependent processes running at the interface between molten steel and functionalizes alumina filters were investigated. The first process was characterized by a reactive behavior of the filter, i.e. polycrystalline alumina structures resulting from heterogeneous nucleation formed on an in-situ formed layer on the filter surface as a result of dissolution and precipitation reactions. Thereby, carbon and gas phases from the carbon-bonded filter material, dissolved oxygen of the steel, iron as catalyst, and probably endogenous inclusions from the steel were involved. Likely due to sintering of the coating material, these interactions stopped and the filter switched to an active behavior. During that stage, endogenous inclusions from the steel deposited on the resulting polycrystalline alumina structures, as alumina inclusions are attracted by alumina of the filter surface. [18]

Clearly we could show that an increased amount of carbon in the coating influenced these stages due to accelerated interactions as well as the presence of more impurities in the coating. If that affected the deposition of endogenous inclusions, cannot be stated at the present, but will be clarified in future investigations.

Our results implicate that the porous structure of the coating should be essential to provide the filter/steel interface with sufficient carbon and gaseous phases to trigger the interactions, which is in excellent agreement with the literature.

ACKNOWLEDGEMENTS

The authors would like to thank the German Research Foundation (DFG) for supporting these investigations in terms of the Collaborative Research Centre 920 “Multi-Functional Filters for Metal Melt Filtration – A Contribution towards Zero Defect Materials”, Subprojects A01, A03, A06, and C01. The authors also would like to acknowledge the support of G. Schmidt and H. Berek.

REFERENCES

[1] Zhang L, Thomas BG. Inclusions in continuous casting of steel. XXIV National Steelmaking Symposium, Morelia, Mich, Mexico. 26-28, Nov. 2003:138–183.

[2] Morgan E. Analyzing steel alloy filtration. Mod Cast. 2003;93:42–45.

[3] Krewerth D, Lippmann T, Weidner A, et al. Application of full-surface view in situ thermography measurements during ultrasonic fatigue of cast steel G42CrMo4. Int J Fatigue. 2015;80:459–467.

[4] Olson III RA, Martins LCB. Cellular ceramics in metal filtration. Adv Eng Mat. 2005;7:187–192.

[5] Emmel M, Aneziris CG. Functionalization of carbon-bonded alumina filters through the application of active oxide coatings for steel melt filtration. J Mater Res. 2013;28:2234–2242.

[6] Dudczig S, Aneziris CG, Emmel M, et al. Characterization of carbon-bonded alumina filters with active or reactive coatings in a steel casting simulator. Ceram Int. 2014;40:16727–16742.

[7] Storti E, Emmel M, Dudczig S, et al. Development of multi-walled carbon nanotubes-based coatings on carbon-bonded alumina filters for steel melt filtration. J Eur Ceram Soc. 2015;35:1569–1580.

[8] Storti E, Dudczig S, Schmidt G, et al. Short-time performance of MWCNTs-coated Al2O3-C filters in a steel melt. J Eur Ceram Soc. 2016;36:857–866.

[9] Poirier J, Thillou B. Contribution of the Refractory Material of Submerged Nozzles to Clogging. Stahl und Eisen Special. 1994;Oct.:114–118.

[10] Salomon A, Emmel M, Dudczig S, et al. Dynamic, in situ generated interfaces between carbon-bonded alumina filters and steel during spark plasma sintering/field-assisted sintering. Adv Eng Mat. 2013;15:1235–1243.

[11] Schwartzwalder K, Somers AV. Method of making porous ceramic articles. US patent 3,090,094. 1961 Feb 21.

[12] Emmel M, Aneziris CG. Development of novel carbon bonded filter compositions for steel melt filtration. Ceram Int. 2012;38:5165–5173.

[13] Emmel M. Development of active and reactive carbon bonded filter materials for steel melt filtration (PhD thesis). Freiberg, Germany: TU Bergakademie Freiberg; 2014.

[14] Fruhstorfer J, Schafföner S, Aneziris CG. Dry ball mixing and deagglomeration of alumina and zirconia composite fine powders using a bimodal ball size distribution. Ceram Int. 2014;40:15293–15302.

[15] Dekkers R, Blanpain B, Wollants P, et al. Non-metallic inclusions in aluminium killed steels. Ironmaking & Steelmaking. 2002;29:437–444.

[16] Zienert T, Dudczig S, Fabrichnaya O, et al. Interface reactions between liquid iron and alumina-carbon refractory filter materials. Ceram Int. 2015;41:2089–2098.

[17] Lee YS, Jung S-M, Min D-J. Interfacial reaction between Al_2O_3–C refractory and Al killed steel. Ironmaking & Steelmaking. 2014;41:286–291.

[18] Aneziris CG, Schröder C, Emmel M, et al. In situ observation of collision between exogenous and endogenous inclusions on steel melts for active steel filtration. Metall Mater Trans B. 2013;44:954–968.